



WaveComBE

mmWave Communications in the Built Environments

WaveComBE_D2.1

Report on scattering model of mmW: Characterization and modelling of human body scattering
in mmWave in-building channels

Version v1.0

Date: 2019/09/29

Document properties:

Grant Number:	766231
Document Number:	D2.1
Document Title:	Report on scattering model of mmW: Characterization and modelling of human body scattering in mmWave in-building channels
Partners involved:	Polytechnic University of Valencia- Spain
Authors:	Narcís Cardona Marcet , Jhoan Samuel Romero Peña
Contractual Date of Delivery:	2019/09/29
Dissemination level:	CO ¹
Version:	1
File Name:	WaveComBE D2.1_v1.0

¹ CO = Confidential, only members of the consortium (including the Commission Services)

PU = Public

Table of contents

- 1. Summary..... 4**
- 2. Introduction 4**
- 3. Scattering effects of the Human Body 5**
 - a. mathematical analytical model..... 5**
 - b. MATLAB Implementation and Simulations 7**
 - c. Unity implementation..... 8**
 - d. Simplification Geometry Measurements 11**
 - e. Human Body Measurements..... 12**
 - f. Conclusions..... 15**
- 4. Passive Reflector 15**
 - a. Conclusions..... 19**
- 5. Future Work 20**
- 6. References..... 20**

List of Figures

Figure 1. DKE Model.....	5
Figure 2. DKE Model MATLAB Implementation, simplified geometrical shape.....	7
Figure 3. Electromagnetic Simulation Software CST,(a) Human Body 3D Model , (b) Human body concealment Results	8
Figure 4. Electromagnetic Simulation Software CST, (a) Human body 3D Model Unity “Red Point = Tx / Blue Point = Rx”, (b) Tx radiation towards the Human Body (Ray-Tracing Technique), (c) Tx-Rx final paths to compute the Knife-Edge model, (d) Tx single axis radiation	9
Figure 5. Unity Platform, (a) Indoor scenario with human body, Rx antenna behind body, (b) Entire amount of rays that were used to develop the Ray-Tracing Technique, (c) Resulting Tx-Rx final paths to compute the Knife-Edge model	10
Figure 6. Geometrical models simplifications to the goal (DKE).....	11
Figure 7. Basic geometrical shape scenario	11
Figure 8. Measurement set-up (human body)	12
Figure 9. Measurement cross-section scenario and measurement real scenario (See Figure 7).	12
Figure 10. Equivalent far field concealment of the human body vs geometrical screen equivalent.....	13
Figure 11. Measurement cross-section scenario with the mannequin with clothes and its equivalent screen (Edge-Projection = Knife-Edge Equivalent) (See Figure 5).....	14
Figure 12. Equivalent far field concealment of the human body vs geometrical screen equivalent.....	14
Figure 13. Conference room scenario, with reverberant antennas.....	16
Figure 14. Specular reflector radiation pattern	17
Figure 15. Different types of surfaces tested.....	17
Figure 16. Optimal Reflector Surface for homogenous radiation pattern (a) tilt : -10° , (a) tilt : 0° , (a) tilt : 10° ,	18
Figure 17. Diffuse reflector radiation pattern with different angles of incidence, (a) with incidence angle at 45° , (b) with incidence angle at 35° to 55°	18
Figure 18 . (a) Measurement set-up reflector antenna (b) Radiation pattern of the passive Reflector	19

1. Summary

In the new generation of 5G mobile radio systems and due to the growing demand of higher bandwidths, it is essential to exploit the millimeter wave band (mmWave) (30 GHz – 60 GHz). Therefore it is essential to rigorously characterize the mobile radio channel in this frequency band, in order to avoid unwanted fading that considerably affects the signal power and increases the noise level.

These new technologies are anticipated to be deployed in various environments such as fixed links, and short range outdoor and indoor environments. In indoor environments, there will be more demand in the short term especially in auditoriums of conferences, and meeting rooms. This frequency range suffers from high free space propagation loss, which limits the power that the mobile terminal can radiate to establish a bidirectional link with the base station. Therefore, initially we consider indoor environments where the transmission range is limited to a few meters.

Indoor environments however, present other challenges due to the presence of obstacles which are electrically large at this frequency range. Therefore, it is necessary to evaluate all the obstructions that affect the propagation of the signal at mmWaves. One of the main obstacles in these interior environments is the human body because of its electrical size and the tissues of the body are an absorbent material at this frequency range. In addition, humans present as mobile obstacles; and hence generate rapid and unexpected fades that considerably alter the propagation of the mmWaves signal. Therefore, in this study we focus on characterizing the scattering effect generated by the human body and study how to mitigate it, in order to characterize the radio channel in mmWaves in a realistic and efficient manner.

2. Introduction

It is important to characterize the human body effects on the propagation of millimetre waves as it is one of the most intrusive elements in the behaviour of the propagation channel for future 5G cellular systems. It is therefore, essential to have a versatile mathematical model that can be easily implemented in any proprietary or free license platform.

For this reason, throughout the literature the issue to characterize the scattering effects of the human body in this frequency range has been addressed with different mathematical models with some more complex than others such as: the screen model and conductive wedge “conducting screen and wedge models (UTD)” [1], the circular cylinder model “circular cylinder model (GTD)” [2], electromagnetic field solver (MoM) [3], numerical integration [4], measurement-based model [5], and the mm-Magic project model “mm-Magic project model” [6].

All these mathematical models have the peculiarity that of a simplified morphology of the human body with simple geometric shapes [7], which is unrealistic despite obtaining very accurate measurements of reality. However, it is important to note that these results are only valid in very

specific circumstances where the human body is static and rigid with a predetermined antenna position and in anechoic chambers.

According to the previous premise, it is important to use a more flexible mathematical model that allows addressing the problem of the characterization of the scattering effect of the human body regardless of its environment, in an efficient and realistic way. Therefore, according to the research articles and our preliminary results we can affirm that the dispersive effect of the human body presents high attenuation which in some cases can be up to 50 dB, even for a single human body. For this reason, it is essential to investigate alternative strategies to avoid these losses, without altering the normal dynamics of the movement of people in these closed environments.

3. Scattering effects of the Human Body

In this study, we are considering the effect human body blockage on millimetre wave propagation in indoor environments. In this scenario the human body is modelled as a non-static obstacle that is electrically large enough to generate temporary variations [8, 9] of the channel as it moves within the environment. It is worth noting that the effect of human body blockage is integrated into the channel model as part of its dynamic behaviour, according to the body movement and morphology.

a. mathematical analytical model

The mathematical model that we propose for the human body is the simplified mathematical model of the Double Knife Edge (DKE) (See Figure 1), which is the best reported model in the literature to characterize this type of phenomenon. It is the most computationally efficient method with comparable results similar to the results of the most complex mathematical models.

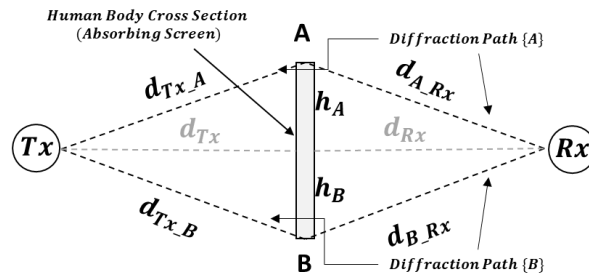


Figure 1. DKE Model

The DKE mathematical model gives the normalized field diffracted at the Rx position, according equation (1):

$$\frac{E}{E_0} = \left(\frac{1+j}{2} \right) \left[\left(\frac{1}{2} - C(v) \right) - j \left(\frac{1}{2} - S(v) \right) \right] \quad (1)$$

Where $C(v)$ and $S(v)$ are cosine and sine Fresnel integrals and the parameter (v) , given in equation (2) is defined as the ratio between the different path lengths from the blocking element edges to the transmitter and receiver, and quantifies the diffraction concealment of the obstacle:

$$v = \pm h \sqrt{\frac{2}{\lambda}} \left(\frac{1}{d_{Tx}} + \frac{1}{d_{Rx}} \right) \quad (2)$$

where λ is the wavelength, d_{Tx} is the distance from the transmitter (Tx) to the blockage absorbing screen, d_{Rx} is the distance from the receiver (Rx) to the blockage absorbing screen, and h is the obstruction/shadow height produced by the obstacle (see h_a and h_b in Figure 1). The v parameter indicates how the incident field is diffracted depending on the amount of shadowing generated by the absorbing screen, which directly depends on the Fresnel radius. The sign uncertainty of the parameter (v) depends on the visibility between the T_x and R_x , and whether the obstacle is within the influence zone of the first Fresnel radius or not. Therefore, in a LOS scenario there is a negative concealment $v(-)$, while for NLOS the concealment is positive $v(+)$.

The DKE diffraction model described above does not consider the polarization of the incident wave, because the human body model is expressed as an absorbing screen. Therefore, it will be necessary to calculate the minimum electrical dimensions of the human body geometric model to assume that polarization is not influencing the far field estimations.

As shown in Figure1, the DKE model calculates two diffraction paths independently, with the reference line-of-sight field given by equation (3):

$$E_O = \frac{\lambda}{4\pi(d_{Tx}+d_{Rx})} e^{-j2\pi\frac{(d_{Tx}+d_{Rx})}{\lambda}} \quad (3)$$

Moreover, the total field at the receiver (Rx) is given in equation (4):

$$E_T = E_{2KE} = E_A e^{-j2\pi\left(\frac{\Delta d_A}{\lambda}\right)} + E_B e^{-j2\pi\left(\frac{\Delta d_B}{\lambda}\right)} \quad (4)$$

where E_A and E_B are diffracted fields observed at the receiver (Rx) and Δd_A and Δd_B are given by equations (5) and (6), respectively:

$$\Delta d_A = (d_{Tx-A} + d_{A-Rx}) - (d_{Tx} + d_{Rx}) \quad (5)$$

$$\Delta d_B = (d_{Tx-B} + d_{B-Rx}) - (d_{Tx} + d_{Rx}) \quad (6)$$

It is worth noting that the diffracted field in each sub-path can have different types of obstructions that will determine the sign of the (v) parameter and the degree of obstruction will depend on the paths to the edges of the obstructing object.

One of the advantages of using this simple model is that it can be extended to characterize multiple diffraction in indoor scenarios where there will certainly be several people and obstacles shadowing the propagation paths.

b. MATLAB Implementation and Simulations

The DKE model was initially implemented with MATLAB in order to determine its viability (See Figure 2), not only to characterize a single obstacle “Human Body” but also to characterize multiple obstacles as in a real scenario.

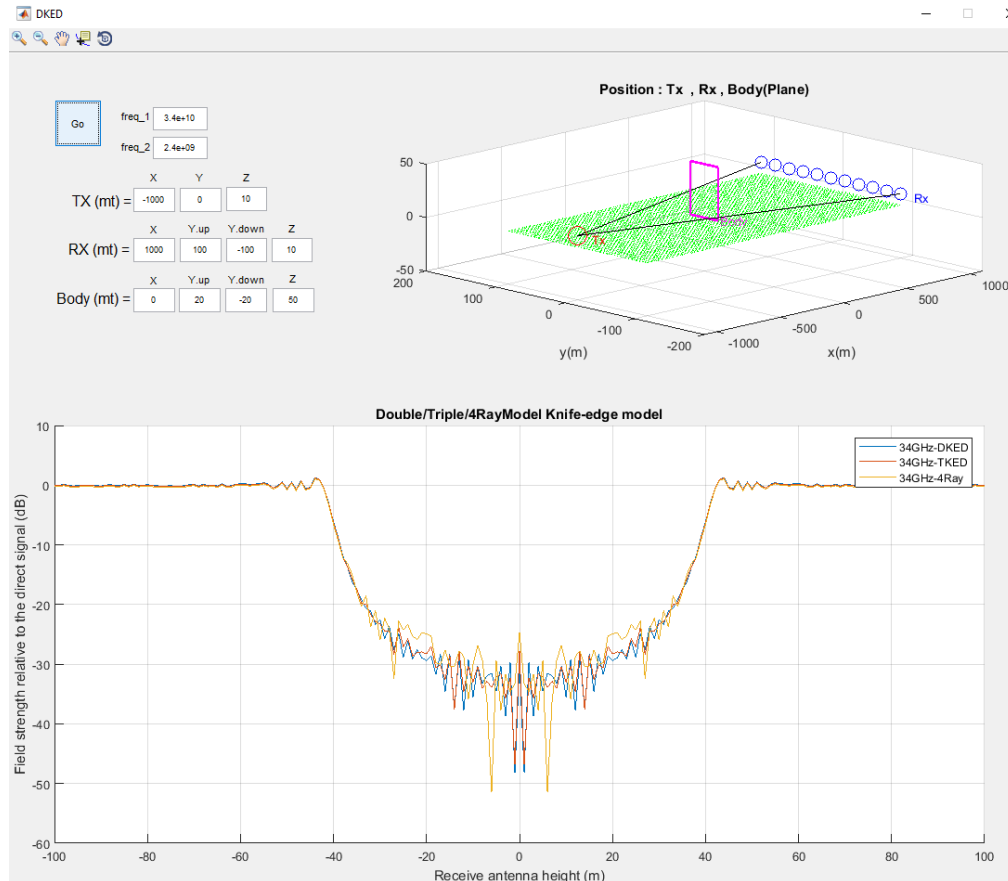


Figure 2. DKE Model MATLAB Implementation, Simplified geometrical shape

Due to the mathematical and geometric restrictions that arise from the simplicity of the DKE model, it was necessary to establish the limits of its applicability and to determine its viability in the mmWave band. According to these restrictions some simplifications have also been proposed to implement this model easily in any software platform for complex indoor environments.

The following are the identified applicability limits [7] to implement the DKE (DKE) model to characterize scattering of the human body in the mmWave band:

1. The minimum electrical dimension of the cross section of any part of the human body must be $\geq 6\lambda$.
2. The minimum electrical distance between the human body and the antennas must from $d_{Tx/Rx} \geq 10\lambda$
3. The antenna polarization in the diffracted field only is relevant when the electrical dimension of the human body is $< 10\lambda$.

4. The polarization influence in the DKE implementation is relevant with lower electrical dimensions (cross section) of the human body less than 10λ .

In order to perform this analysis, simulations were carried out in both MATLAB and in the CST electromagnetic analysis platform and preliminary results can be seen in Figure 3.

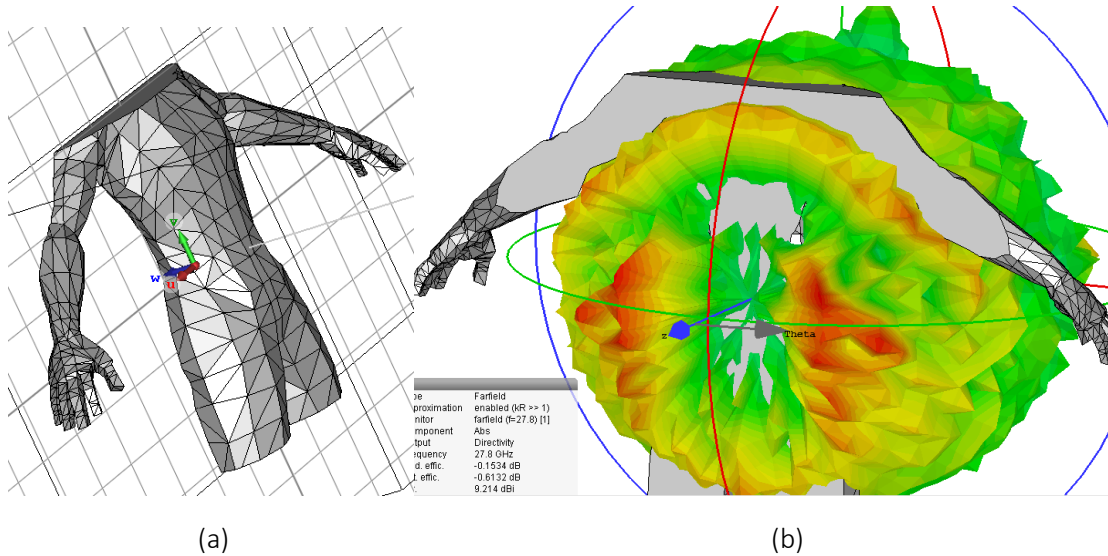


Figure 3. Electromagnetic Simulation Software CST, (a) Human Body 3D Model , (b) Human Body concealment Results

The results of the analysis were presented as a Technical Document at the meeting of (IRACON-COST ACTION CA15104 - Dublin-Ireland, TD (19)09089) and a paper at the 13th Antennas and Propagation European Conference (EUCAP), 2019 [7].

c. Unity implementation

In this investigation, we implemented the mathematical model with the Unity gaming platform. This platform was chosen since it is open access and it is quite versatile. It also allows us to develop a ray-tracing technique with its collision management tool that is normally used for game mechanics.

Using Unity collision management tools, we implemented our mathematical model with a logic of ray tracing, based mainly on the relative distances between the edges of the object(s) and the position of the transmitter and receiver, considering the DKE applicability limits of the previously conducted study.

To carry out this implementation, approximately 10,000 lines of C # code were created, which were necessary to implement the DKE model in a complex “multiple obstacles” environment. The results from this model are displayed in Figures 4 and 5 and show that it is the most suitable to characterize the radio channel in the millimetre wave band in indoor environments, focusing especially on the effects of the human body. It is also important to emphasize that this DKE model can be used to characterize any type of obstacle that is composed of a fully absorbent or reflective material in the millimetre frequency range.

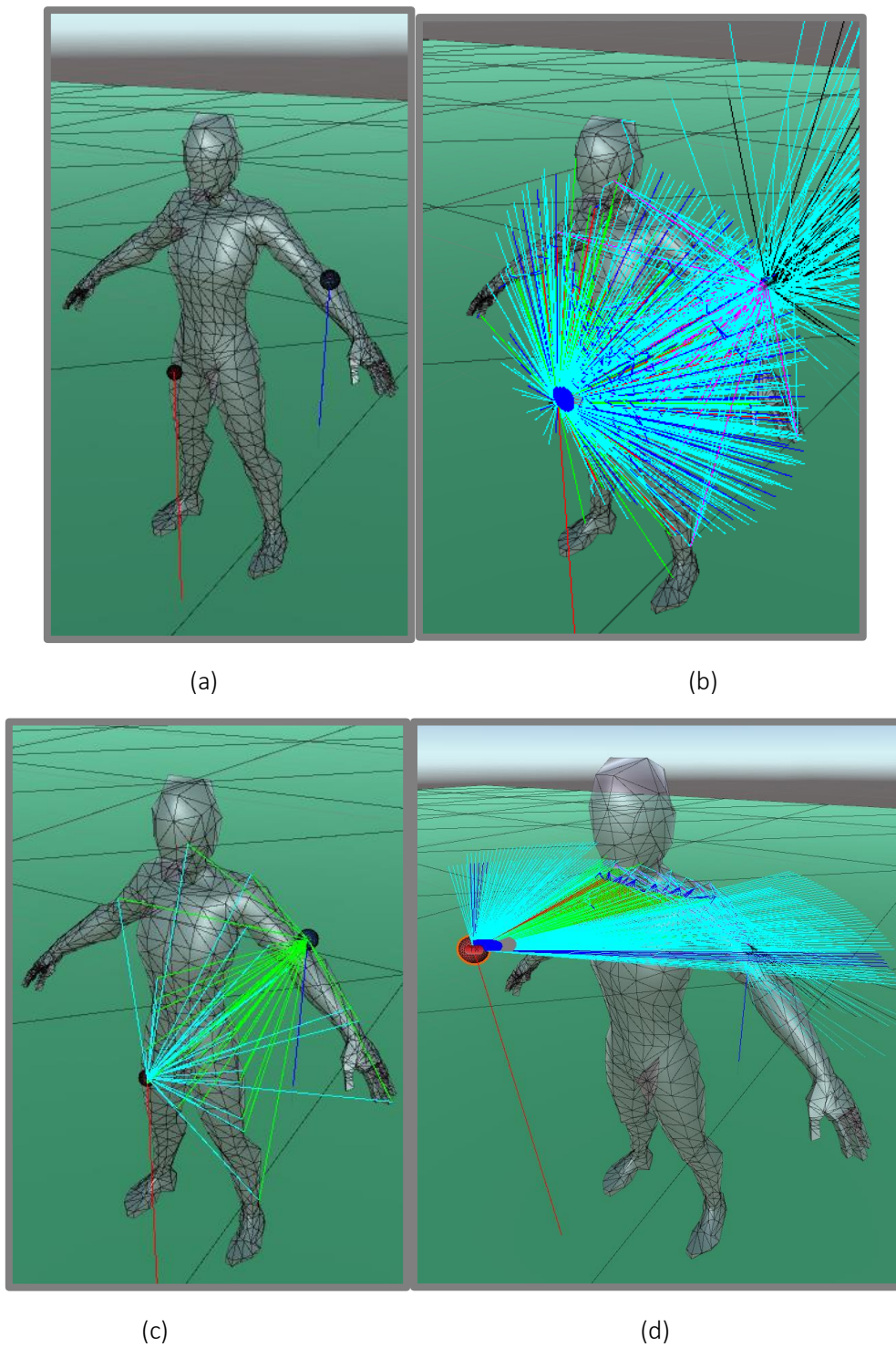
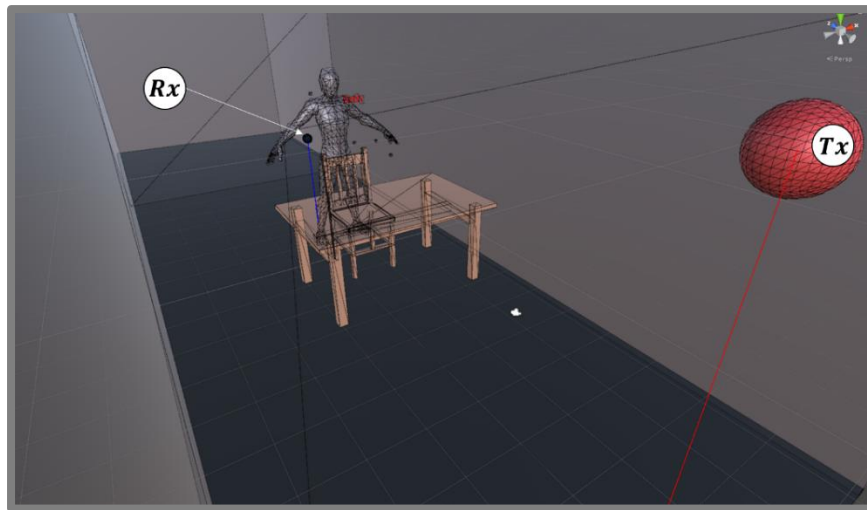
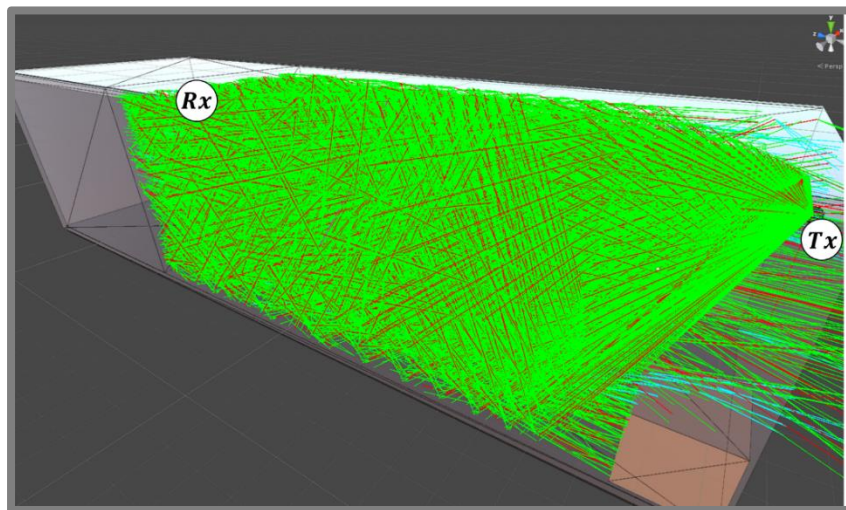


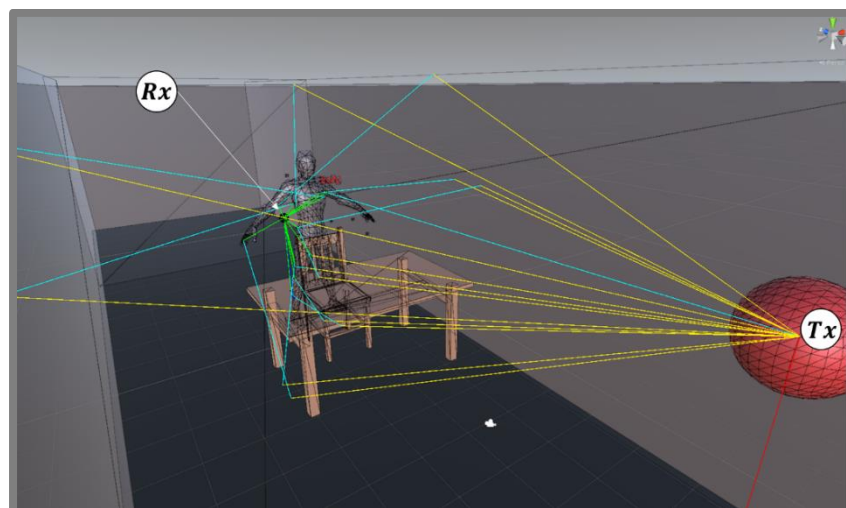
Figure 4. Electromagnetic Simulation Software CST, (a) Human body 3D model Unity “Red Point = Tx / Blue Point = Rx”, (b) Tx radiation towards the Human Body (Ray-Tracing Technique), (c) Tx-Rx Final paths to compute the Knife-Edge model, (d) Tx single axis radiation



(a)



(b)



(c)

Figure 5. Unity Platform, (a) Indoor Scenario with Human Body, Rx antenna behind Body, (b) Entire amount of rays that were used to develop the Ray-Tracing Technique, (c) Resulting Tx-Rx Final paths to compute the Knife-Edge model

d.Simplification Geometry Measurements

At this stage of the investigation, and according to the applicability limits described in [7], the human body geometry was simplified (See Figure 6). This simplification allows calculating the far field obstruction of an equivalent obstacle, which has the same diffraction effect as the concealment generated by the complex morphology of the human body with tissues. This is the fundamental premise on which the Knife-Edge Model is based, which was used in the implementations in the MATLAB-Unity.

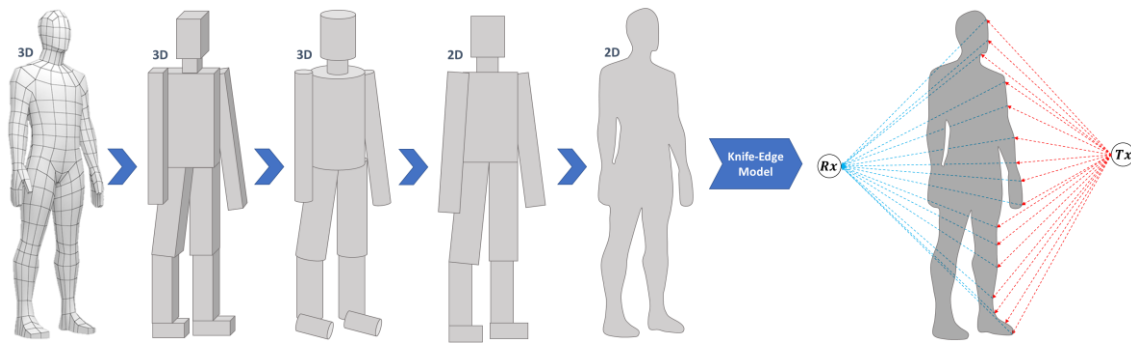


Figure 6. Geometrical Models Simplifications to the goal (DKE).

To confirm the premise of the proposed geometric simplification, it was necessary to perform measurements with the basic geometric shapes (See Figure 7), which according to the executed simulations and implementations, these results must be equivalent, as shown in Figure 10.

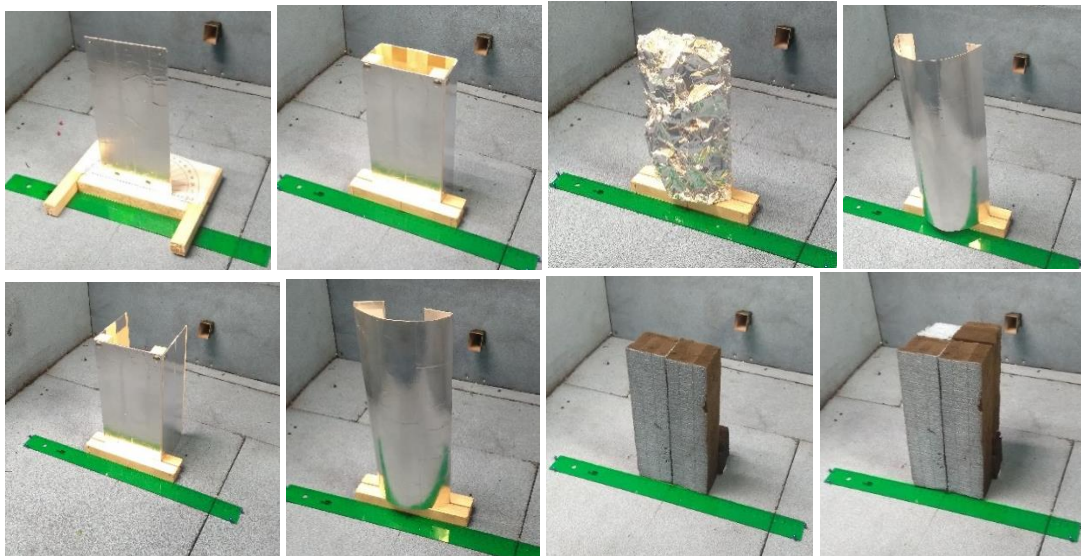


Figure 7. Basic Geometrical Shape Scenario

In conclusion, considering the different geometric shapes at different wavelengths, the DKE mathematical model is suitable to characterize the human body considering the limits of applicability that were proposed regarding the minimum electrical dimensions of the obstacle “Human Body”.

With these conclusions in mind, we also performed measurements directly with a human body and its metallic geometric equivalent (See Figure 8), in order to reaffirm the conclusions made

on a small scale. With this plan we fully confirm that the proposed model is valid to characterize the human body in the mmWave band.

e. Human Body Measurements

In this measurement set-up, we changed the position of the antennas (Tx-Rx) that are always aligned with respect to each other; in order to characterize the obstruction of the obstacle (Diffraction Losses) (See Figure 8). In this case, these would be the reference person, the contour metallic model at 1:1 scale of the reference person's body (See Figure 8.b), and finally the mannequin where we will verify the influence of the clothing in the concealment (See Figure 11). In all the measurements, we use as a reference the applicability limits identified in [7].

The measurements were performed with a VNA by measuring the S21/S12 parameter at different heights (Head 154 cm, Shoulders 140 cm, Upper Torso 130 cm, Half Torso + Arms 100 cm) to analyse several cross sections to evaluate different types of tissues of the human body and to determine if there are relevant differences between them. The resulting scattering behind the body is displayed in Figure 10 where the results were obtained directly with the human body (See Figure 9.c) and its equivalent metallic shape (Outline Model) (See Figure 9.d)

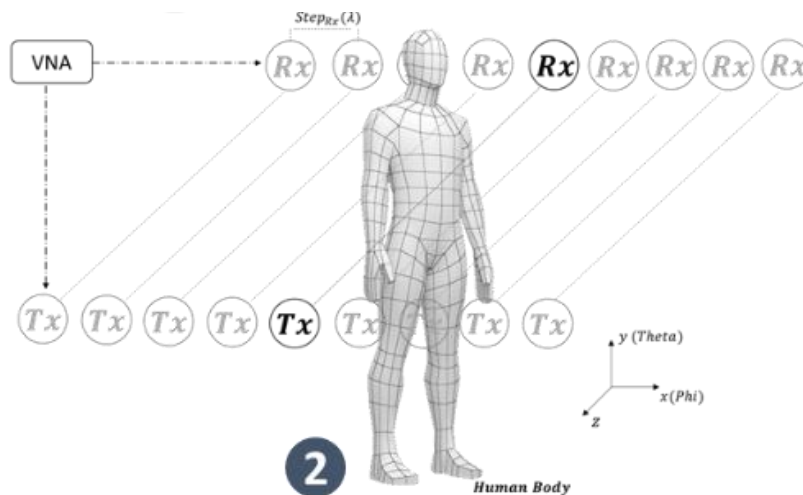


Figure 8. Measurement Set-Up (Human Body)

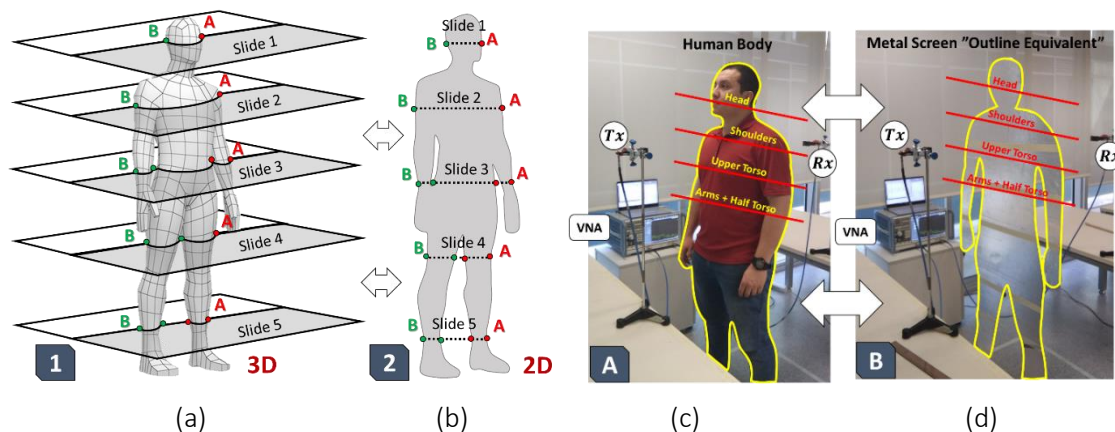


Figure 9. Measurement Cross-Section scenario and Measurement Real Scenario (See Figure 7).

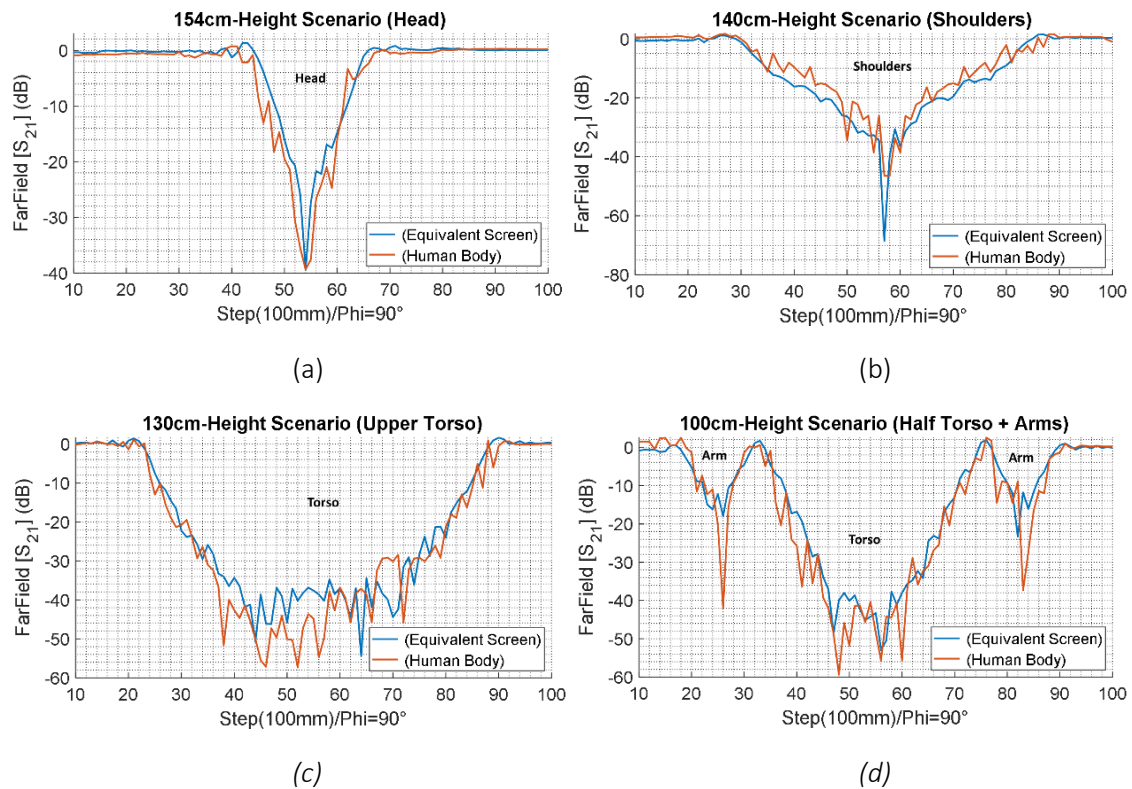


Figure 10. Equivalent far field concealment of the human body vs Geometrical screen equivalent.

According to the results in Figure 10, we confirm that the geometric equivalent made with a metallic screen as illustrated in Figure 9.d is equivalent to the human body, if we just retain its equivalent edges (Edge-Projection [7]) between the Tx/Rx (See Figure 9 “Points A-B”). This is very useful because it considerably simplifies the implementation of the DKE model and the measurements without having a person in a specific place for the measurement campaigns.

In the second analysis and as concluded in the previous measurements, we determined the scattering influence that the clothing could have on the total final concealment of the human body. This is very important to consider, because in the previous analysis the measurements were made directly of the human body with only underwear, something that is not reflected in Figure 8.c for privacy reasons. In this analysis winter clothes are considered, due to the voluminous and density so it is expected to have greater influence on the scattering behaviour in the mmWave (See Figure 11.c).

In this study no measurements were taken directly with the human body since the results indicated that it is not necessary to directly measure the human body, when a geometric equivalent of the metallic screen outline is available.

In this study we used a mannequin coated with a metallic layer as shown in Figure 11.a, which is equivalent to the human body shape and the equivalent of the contour metal screen model (See Figure 11.b), according to [7] and previous conclusions.

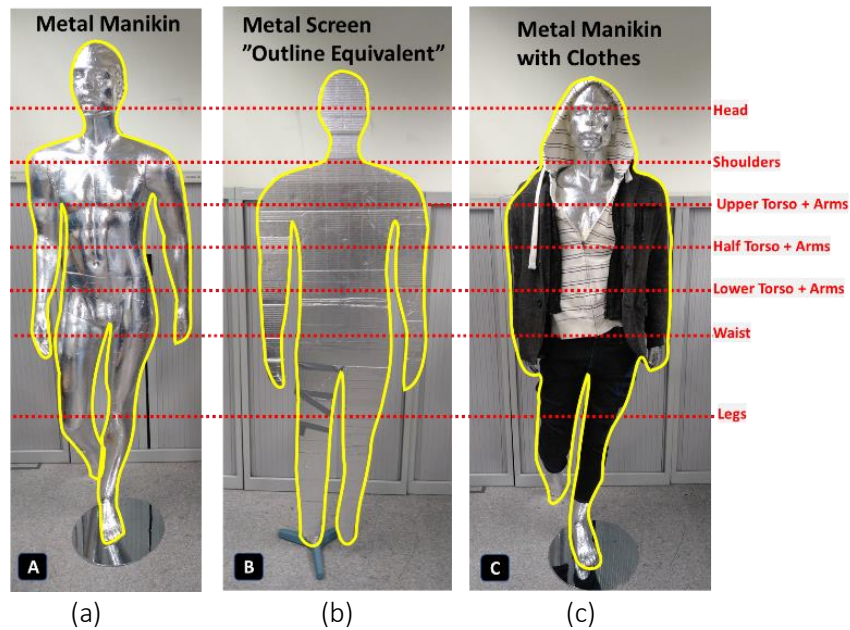


Figure 11. Measurement cross-section scenario with the mannequin with clothes and its equivalent Screen (Edge-Projection = Knife-Edge Equivalent) (See Figure 5).

According to the results in Figure 12; the geometric equivalent "metal outline screen" is equivalent to the complex three-dimensional geometrical form of the mannequin, only if the same edge projection of the body is preserved with precision [7] (Figure 9.a-b "Points A/B"). Thus the conclusions in this section will be extrapolated to the scattering effects of the human body.

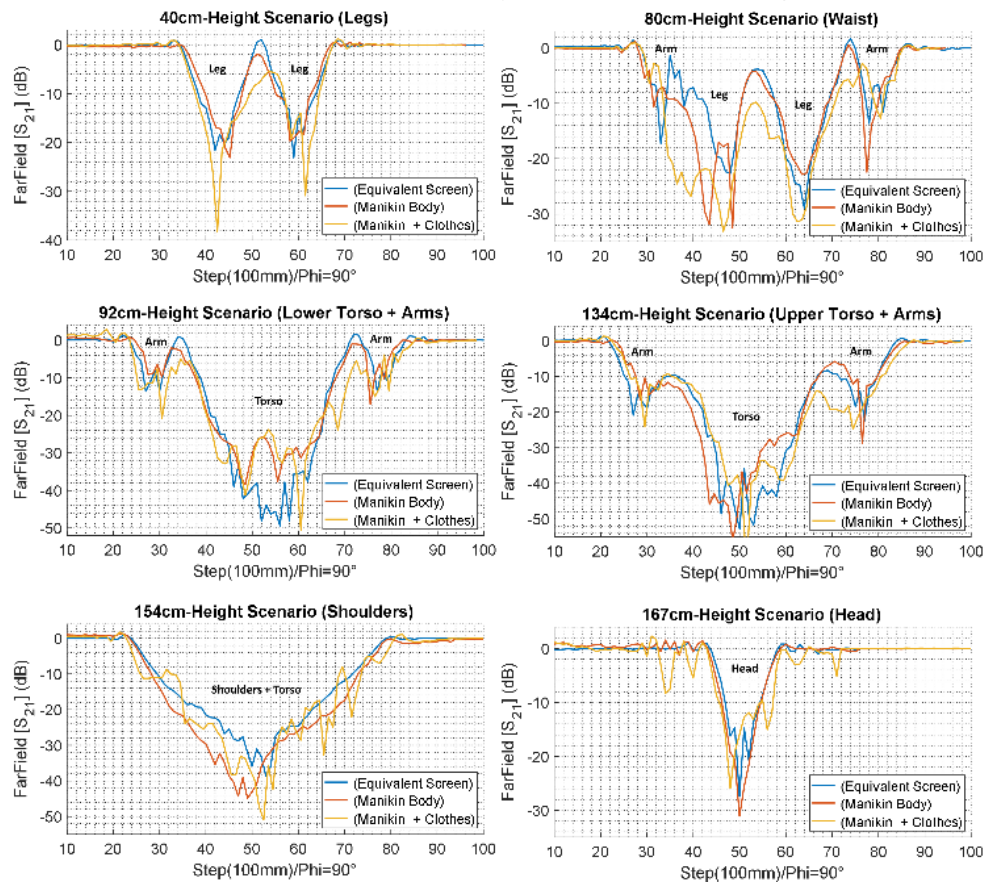


Figure 12. Equivalent far field concealment of the human body vs geometrical screen equivalent.

f. Conclusions

In summary, the conclusions of the study of the scattering effects of the human body are:

1. To correctly characterize the concealment of the human body, we must identify the edge-projection, which depends on the position/orientation of the Tx/Rx that will determine the concealment behaviour, independent of its fixed physical dimensions, in the range of 30 GHz to 40 GHz, according to measurements and simulations.
2. The complex geometric shape of the human body can be simplified by its bidimensional geometric equivalent with the same edge-projection of a metal screen. This validates the results obtained in [7] and confirms the applicability of the DKE “DKE model” to characterize the human body scattering effects in a simulation environment efficiently and to simplify taking measurements without people.
3. The clothing has a slight dispersive effect on the final concealment generated by the human body. Therefore, to characterize the human body scattering effects with the knife-edge model, clothing could be discarded and it is only necessary to consider the human body as a totally absorbing obstacle at mm-Wave or totally reflective in the case of its geometric equivalent with the same edge-projection for measurements.

4. Passive Reflector

As concluded in the first part of the research “scattering effects of the human body” the losses due to the interaction of the human body with the mmWaves (30-40 GHz) are very high around 40-50 dB and are almost impossible to avoid. Due to the normal position of the mobile phone in relation to the human body; trying to propagate the signal in a traditional way using the strategy of re-directing the antenna beam towards the mobile phone is very inefficient, due to the amount of obstacles that exist in this type of indoor environment.

Therefore, all efforts to have a more directive antenna with greater gain and with beam tracking will be in vain, because all that power is going to be lost by the scattering effects of the human body and all the entire environment “Furniture, Floor, Walls, etc...”

Due to all these effects, in this new investigative stage, strategies will be created to avoid these high losses, with antennas at mmWaves. One solution is to design a passive reverberant antenna (Figure 13 - Passive Antenna), which will serve as support for the actual mmWave arrays (Figure 13 - Active Antenna), with the aim of increasing the power level in the indoor environments.

The objective of this reflector antenna is to avoid pointing the beam of the active antenna towards the receiver “Mobile Phone”, but to redirect the beam towards the passive reflector which in principle is a longer path but with lower losses. This is the best cost-benefit solution, to increase the coverage in large indoor environments.

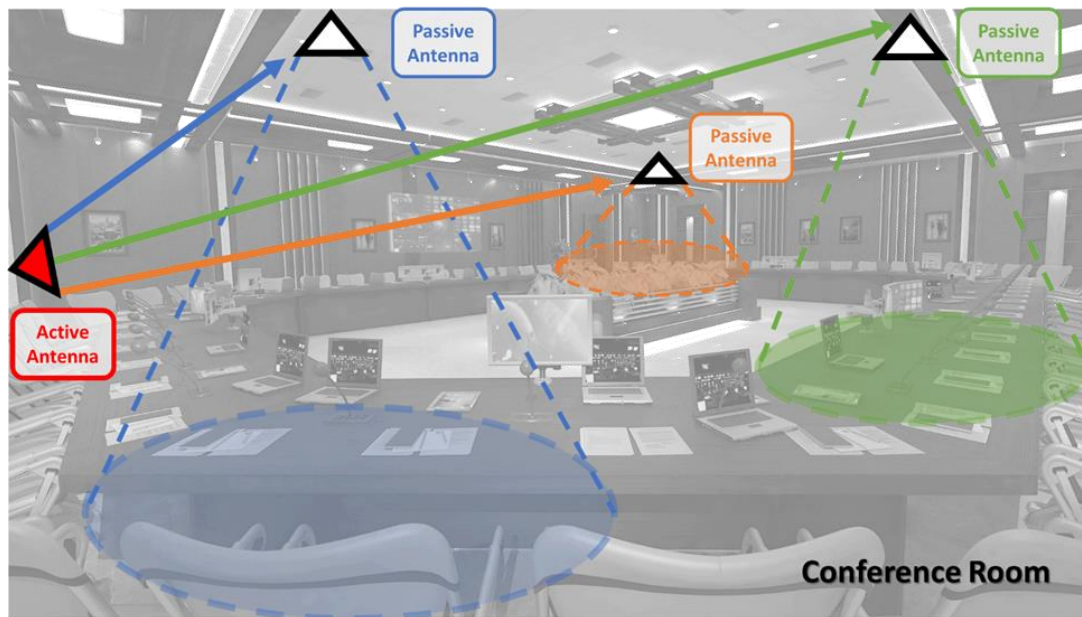


Figure 13. Conference room scenario, with reverberant antennas

Numerous solutions have been proposed throughout the literature to avoid the problems of high signal attenuation in both indoor and outdoor environments. Some of these proposed solutions include beamforming and beam-steering techniques using multiple antennas, high transmit power and high sensitivity receivers, and use of multiple active repeaters. However, all these strategies are very complex and expensive techniques, because the coverage of each base station in the mmWave band would be the equivalent of the current peak cells in the best cases (100 meters). For this reason, to start up a complete network in the mmWave band would result in a high initial monetary investment by the company or country that wants to have it in motion.

In addition to the technical limitations and the coverage that comes with the use of this technology, another big problem is the maximum power allowed to avoid health problems due to the absorption of radiation in the tissue of the human body.

This type of reflector cannot be a flat reflector, because in future 5G mobile systems in the mmWave band they will initially be offered with very directive array antennas in order to counteract the intrinsic losses of free space. For this reason, if a simple flat reflector is used, the output radiation of the reflector “coverage” will depend on the directivity of the antenna and its angle of incidence on the reflector. Therefore, this reflector will have a specular behaviour that is very dependent on the entry conditions (See Figure 14).

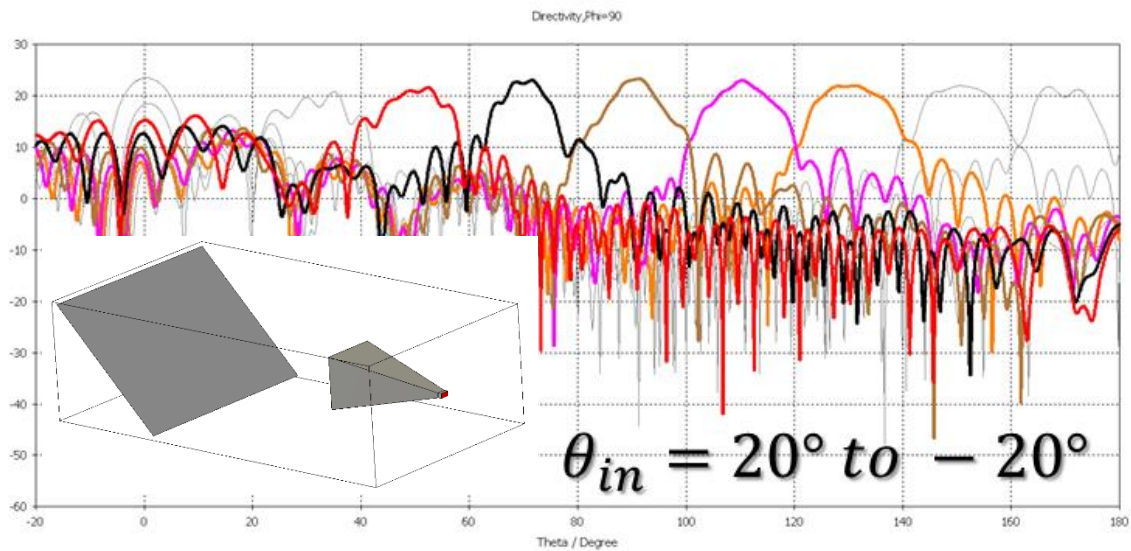


Figure 14. Specular reflector radiation pattern

For the design of this reflector, a rough surface will be designed to allow diffuse reflections in order to increase coverage and to offer an alternative path to the radio link established between the base station and the mobile unit.

For the design of this reflector it was tested with several types of surfaces (See Figure 14) in order to identify the best surface with a diffuse homogeneous behaviour that is easily parameterized according to its roughness and its shape.

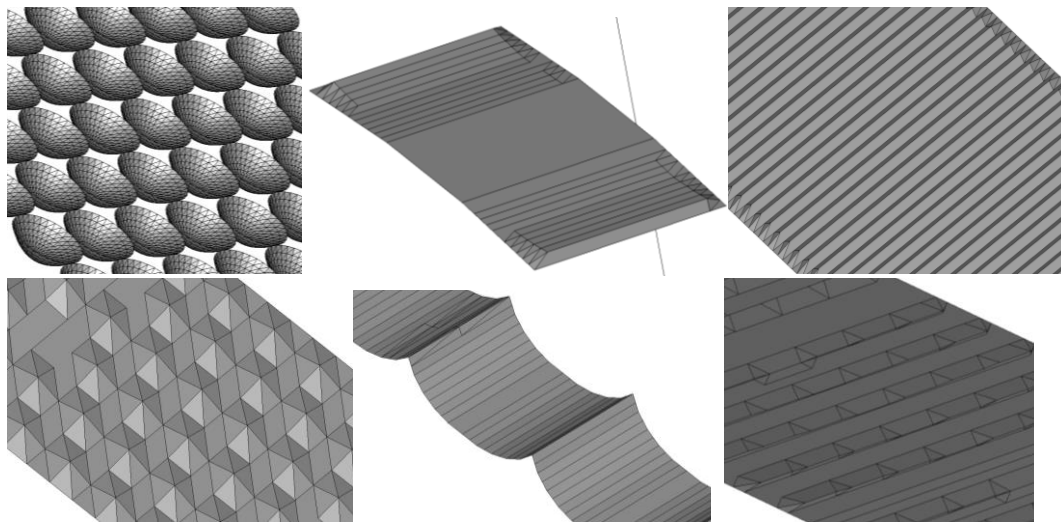


Figure 15. Different types of surfaces tested

Thus, the objective of our reflector will be to homogeneously distribute the energy received over a specific coverage region that will be independent of the angle of incidence on the reflector in order to avoid specular reflection in the output radiation of the reflector.

After testing several surfaces, we identified an optimal surface, which gives a relatively homogeneous diffuse radiation pattern with an opening angle range of approximately 20° (See Figure 16). The convergent coverage zone with different angles of incidence (-10° to 10°),

radiates the same amount of energy over the same area, independent of its angle of incidence 70° to 110° (See Figure 17).

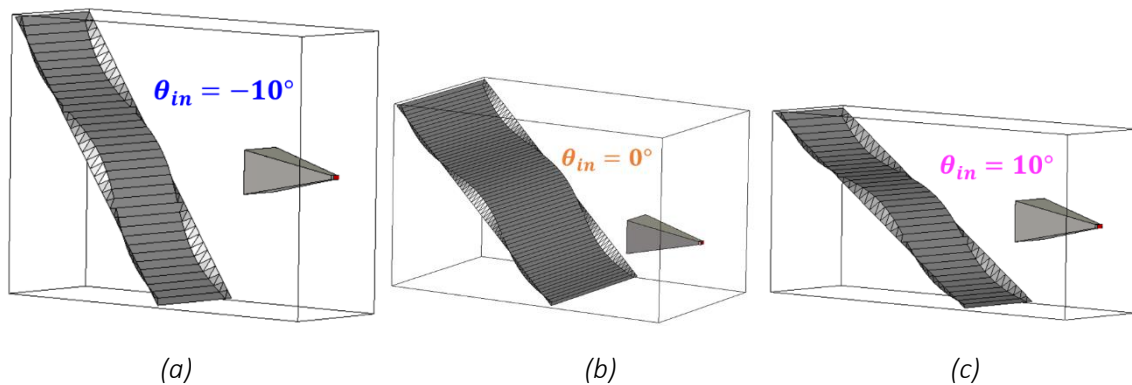


Figure 16. Optimal Reflector Surface for homogenous radiation pattern (a) tilt : -10° , (a) tilt : 0° , (a) tilt : 10° ,

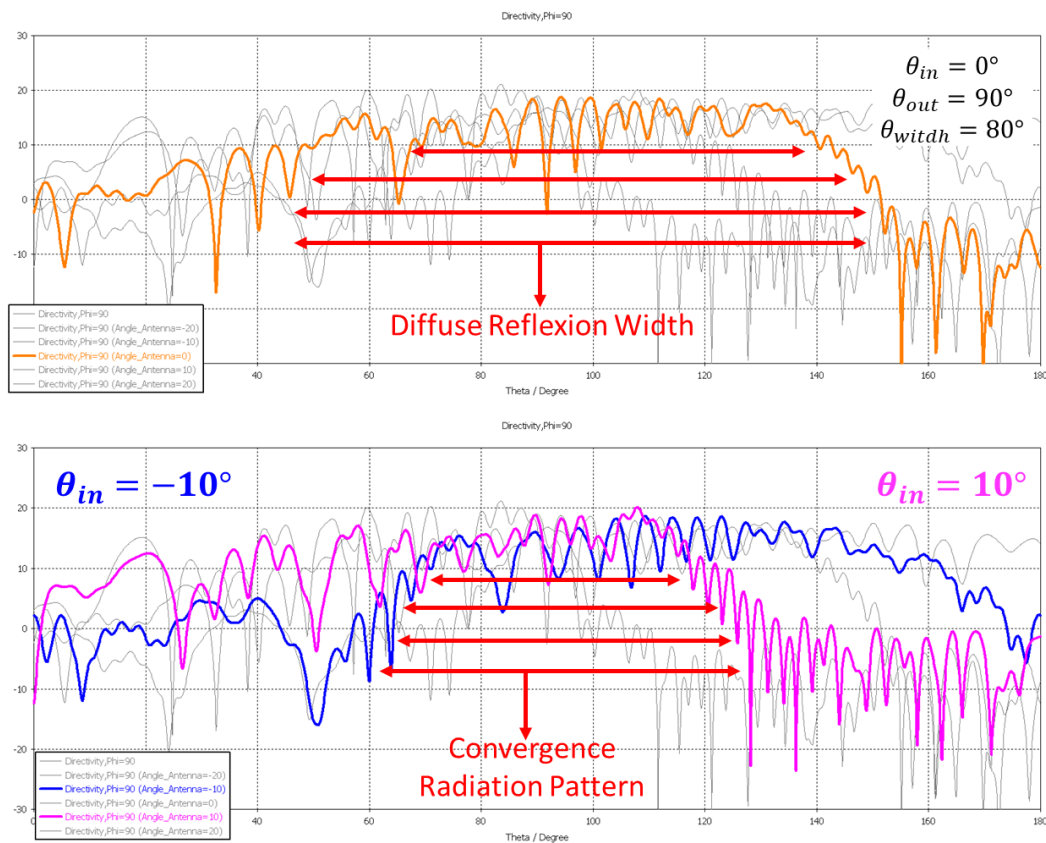


Figure 17. Diffuse reflector radiation pattern with different angles of incidence, (a) with incidence angle at 45° , (b) with incidence angle at 35° to 55° .

To make a fast and economical prototype of this reflector a 3D printer was used, where the antenna was printed with plastic and then was covered with a metallic layer, so that it works as a reflector. This manufacturing process is valid because the depth of penetration in this frequency range is minimal.

Preliminary measurements were made on this antenna with satisfactory results (see Figure 18-19), although we are still in the design process to identify the optimal surface for a reflector bandwidth of 30 to 40 GHz.

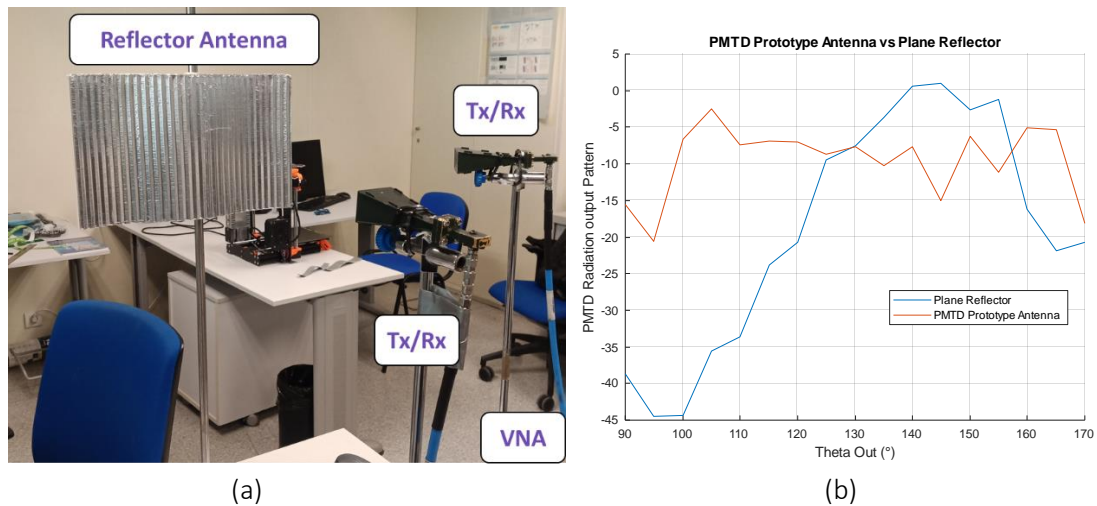


Figure 18. (a) Measurement set-up reflector antenna (b) Radiation pattern of the passive Reflector

a. Conclusions

According to the simulations and measurements, the results so far have been satisfactory. However, these preliminary results are still in need to be refined in both design and manufacture. Currently, as part of the secondment, we are working with our partner GAPWAVES who is interested in the potential of this idea to complement its antennas, in order to guarantee a homogenous distribution of energy in future 5G systems in the mmWave band in indoor environments.

The results of the work carried out thus far on the design of the passive reflector, will be submitted in a paper to the (14th Antennas and Propagation European Conference (EUCAP), 2020).

In addition, currently we are working on the creation of the reflector as a "Passive, Modular, Tetrahedron, Diffuser = PMTD" antenna where it is the same concept, but the idea is to make the modular reflector so that it is easily assembled according to the needs of coverage of the indoor environment and the directivity characteristics of the antenna which is feeding the reflector (See Figure 19).

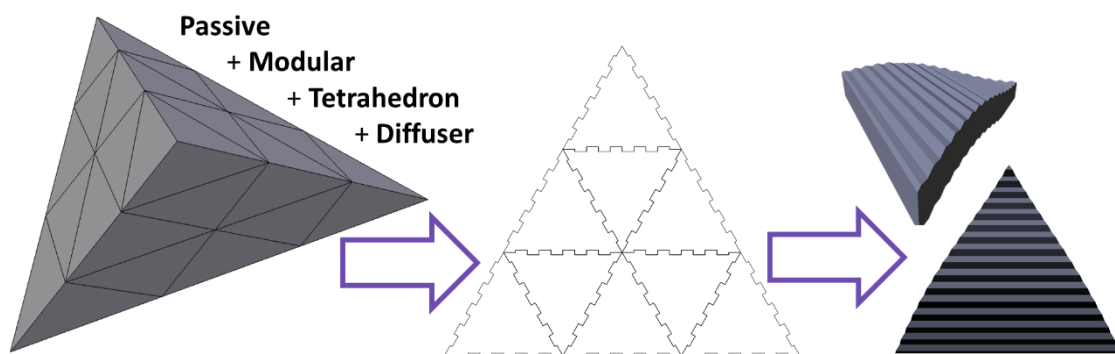


Figure 19. PMTD (Passive, Modular, Tetrahedron, Diffuser) reflector concept

5. Future Work

We are currently working on the design of a specular reflector in the millimetre wave band with the short-term objective to have an operational prototype of the reflector contrasted with measurements. This will then be integrated into the radio network systems in the millimetre wave band proposed by Gapwaves, together with their antenna array.

The reflector will also be integrated into the Unity simulation environment, together with the ray tracing techniques that were addressed in the first part of the research of the characterization of the scattering effects of the human body.

Finally, the goal is to have a proprietary tool that maps any indoor environment in order to identify the best transmitter and reflector antenna positions for optimal coverage in conference rooms.

6. References

- [1] N. Tran, T. Imai, and Y. Okumura, "Study on Characteristics of Human Body Shadowing in High Frequency Bands," 2014.
- [2] M. Yokota, T. Ikegama, Y. Ohta, and T. Fujii, "Numerical examination of EM wave shadowing by human body," *Antennas Propag. (EuCAP), 2010 Proc. Fourth Eur. Conf.*, pp. 4–7, 2010.
- [3] C. Gustafson and F. Tufvesson, "Characterization of 60 GHz shadowing by human bodies and simple phantoms," *Radioengineering*, vol. 21, no. 4, pp. 979–984, 2012.
- [4] A. G. Aguilar, P. H. Pathak, and M. Sierra-Pérez, "A canonical UTD solution for electromagnetic scattering by an electrically large impedance circular cylinder illuminated by an obliquely incident plane wave," *IEEE Trans. Antennas Propag.*, vol. 61, no. 10, pp. 5144–5154, 2013.
- [5] M. Peter *et al.*, "Analyzing human body shadowing at 60 GHz: Systematic wideband MIMO measurements and modeling approaches," *Proc. 6th Eur. Conf. Antennas Propagation, EuCAP 2012*, pp. 468–472, 2012.
- [6] D. Number, P. Name, M. B. Mobile, R. Access, F. Generation, and I. Communications, "Measurement Results and Final mmMAGIC Channel Models Measurement Results and Final mmMAGIC Channel Models," 2017.
- [7] J. Samuel Romero-Peña, Narcís Cardona, "Applicability Limits of Simplified Human Blockage Models at 5G mm-Wave Frequencies", *Antennas and Propagation (EuCAP) 2019 13th European Conference on*, 2019.
- [8] P. Marinier, G. Y. Delisle, and C. L. Despins, "Influence of Human Motion on Indoor Wireless Millimeter-Wave Channel Characteristics," *Ieee*, vol. 18, no. 4, p. S2, 1983.
- [9] X. Chen, L. Tian, P. Tang, and J. Zhang, "Modelling of human body shadowing based on 28 GHz indoor measurement results," *IEEE Veh. Technol. Conf.*, no. 92, pp. 0–4, 2017.